

# CFD BASED ANALYSIS OF VORTEX SHEDDING IN NEAR WAKE OF HEXAGONAL CYLINDER

S.Dave<sup>1</sup>, Dr. B.S More<sup>2</sup>

<sup>1</sup>M.Tech. Scholar, Dept. of Mechanical Engineering, Shri Govindram Seksaria Institute of Technology And Science, Indore, Madhya Pradesh, India

<sup>2</sup>Associate Professor, Dept. of Mechanical Engineering, Shri Govindram Seksaria Institute of Technology And Science, Indore, Madhya Pradesh, India

\*\*\*

## Abstract

Since the discovery of Kármán vortex streets, flow around bluff bodies has garnered a lot of investigation. Studying the vortex behaviour, the distribution of velocity and pressure on body are very important from a practical standpoint. Analysing the unsteady wake behind the body of circular and square geometries has been the subject of in-depth research using numerical techniques like computational fluid dynamics (CFD), in order to forecast the resulting pressure and velocity field around the body. The flow around stationary circular and rectangular/square cylinders has been the subject of extensive study. In contrast to that, only a small amount of research has been done on the flow zone behind hexagonal cylinders. The vortex behaviour including lift, drag and vortex frequency analysis of the 2D hexagon are the subjects of this study.

**Key Words** – Reynolds Number, Strouhal Number, Strouhal Frequency, Vortex Shedding, Lift, Drag

## 1. Introduction

Numerous studies have been conducted on flow around bluff bodies. The flow around sphere, square, rectangular geometries have been the subject of extensive study. Large zones of separation, as seen in Fig. 1, define the flow around a circular body. The boundary layer's separation from the cylinder's surface causes the flow to recirculate. Geometric shape of the bluff body results in non favourable pressure gradient in flow direction. Leonardo Da Vinci most likely pay close attention to creation of swirling patterns in the wakes for the first time in 1504 AD ( Bearman, 1965 ). A more thorough explanation of the flow around a body was published by Reynold.

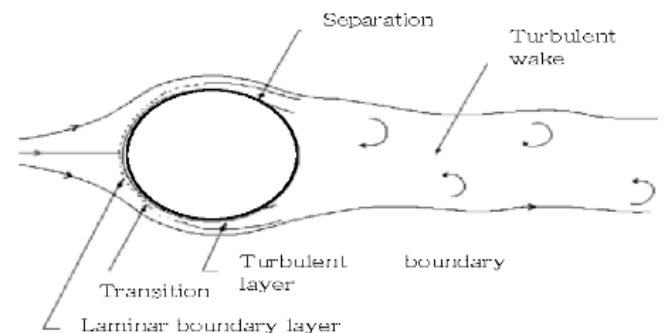


**Figure1** Laminar Boundary Layer Wake Formation

The the synthesis of comparatively slower flowing liquid in the boundary layer, the unfavourable pressure gradient caused by the wake, boundary layer separation, and instability in the flow causes vortex shedding behind bluff bodies. Bloor (1965) found that the near-wake region's length and width had changed. The greatest negative pressure after the body, which all of the various flow regimes share, causes boundary layer separation over over the bluff body's broadest area. At areas where boundary layers separate, shear layers are always formed. Because of the increased flow velocity in the proximity closer to the free stream than it is near the cylinder, which leads to rolling up the shear layers and further leading to vortices creation (Blevins, 1990). Shedding of a vortex occurs as soon as the vortex shear layer contacts with the shear layer on the opposite side, and the vorticity is reduced due to its different sign. Each side of the cylinder goes through this process once, creating a vortex street in the process. The Strouhal number can be used as a non-dimensional expression for the vortex shedding of a motionless cylinder. (Gerrard, 1966).

$$St = f_s U/D$$

Where, St - Strouhal number

U - flow velocity

D - cylinder diameter

$f_s$  - frequency of vortex shedding.

Reynolds number influences how frequently vortices shed in the wake of a cylinder., according to earlier experimental findings (Sumer B.M., 2006)

**Von Karman Vortex** : - The drag and lift force exerted by the fluid on the cylinder, are often separated. Reynolds numbers above 40 cause the flow to oscillate and cause vortex shedding. Because of the periodic variation in the pressure field surrounding the bluff bodies, the force components also start to follow a predictable pattern. The drag and lift forces can be further separated into mean and fluctuation parts for analytical reasons. Whereas mean drag coefficient  $C_D$  varies about its mean value and has a fixed value. In contrast, the mean Force of lift varies around 0 and mean lift coefficient  $C_L$  is nil and varies very less.

The drag force will exert its influence on the cylinder surface in the flow direction according to the size, shape, and orientation of the bluff body. The relationship between the drag force and fluid velocity is defined by the drag coefficient  $C_D$ , which is provided by:

$$C_D = 2 F_D L / \rho L U^2 D$$

Where,  $\rho$  - fluid density,

$U$  - velocity of fluid flow,

$D$  - diameter of cylinder body,

$L$  - length of cylinder body

$F_D$  - drag force.

Furthermore,  $C_L$ , the lift coefficient, is computed similarly, but it also takes into account the force acting in the direction perpendicular to that of the flow. The lift force, abbreviated  $F_L$ , is word used to describe the force that corresponds to the cross-flow direction.

$$C_L = 2 F_L L / \rho L U^2 D$$

Where  $\rho$  - fluid density

$U$  - velocity of fluid flow,

$D$  - diameter of cylinder body,

$L$  - length of cylinder body

$F_L$  - lift force

Khaledi and Andersson (2011) investigated the vortex structure underlying hexagonal cylinders with faces and corners. Although the small disturbed vortex structures

and the vorticity with extremely erratic flow patterns were downstream of the hexagonal cylinder, subcritical Reynolds numbers allowed for visualisation of the turbulent flow's characteristics. However, there weren't many distinctions between corner orientation and face orientation vortex structures when compared downstream (Khaledi & Andersson, 2011).

Skyscraping buildings, tunnel that float, and frames that support prototype for testing in wind tunnel are a few examples of engineering issues that frequently include polygonal cross-section with  $N \geq 3$  [ $N$  refers to no of side ]. Unfortunately, the literature on cylinder with  $N > 4$  has received far less attention than that on the circular cylinder wake, and the relevant data are rare. The previously recorded data for square and rectangular cylinder are used with approximation whenever new problems regarding cylinder with  $N > 4$  is faced. Even under the identical flow conditions, as will be shown in this study, the fluid parameters associated with cylinder with  $N > 4$  might change dramatically from those associated with a circular or square cylinder in some situations, making this method exceedingly dangerous.

$$Re = \rho V L / \mu$$

$$St = F_{st} L / U_0$$

$Re$  = Reynold Number

$St$  = Strouhal number

$\rho$  = Density of fluid

$\mu$  = Dynamic Viscosity of fluid

$L$  = Characteristic Length

$U_0$  = velocity of the ambient flow

$F_{st}$  = Strouhal Frequency

## 2. Modelling

### 2.1 Design

We have considered the flow across cylinder with corner oriented hexagonal cross-section. All sides of polygon are measured  $L$  with all interior angles measuring 120 degree. Corner orientation is considered as show in figure 2. The cylinder was located  $20L$  from velocity inlet boundary and  $60L$  from pressure outlet boundary, with cartesian coordinates of the system located at centre of the cylinder.

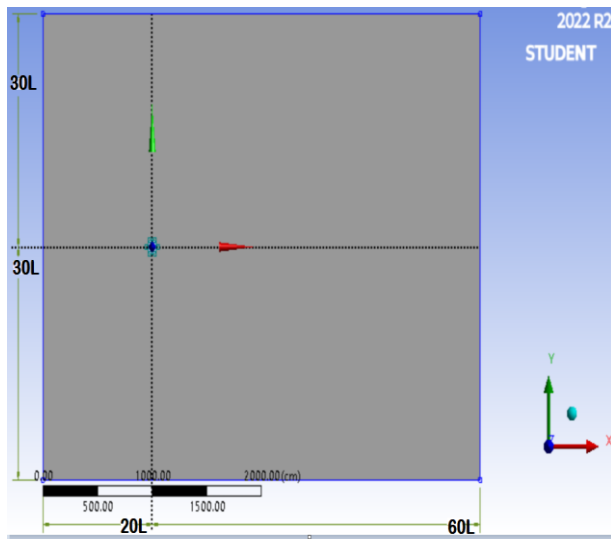


**Figure 2** Schematic of computational dimension for studying the flow past hexagonal cylinder

### 2.2 Meshed Model

The ANSYS 2022R2 student version is used to complete the mesh generation. This software generates finite-element grids in three dimensions and is open-source. For  $Re = 100, 500$ , and  $1000$ , the computational domain is discretized into 143505 grid cells. Six distinct mesh types were examined for the grid independence test. Making our mesh finer may produce different results when we start with a coarse mesh and solve. However, there is a point beyond which, no matter how fine we make it, we won't see any differences in the outcomes. We can then claim to have attained grid independence. The mesh will now be fine enough to record even the most minute aspects of the flow.

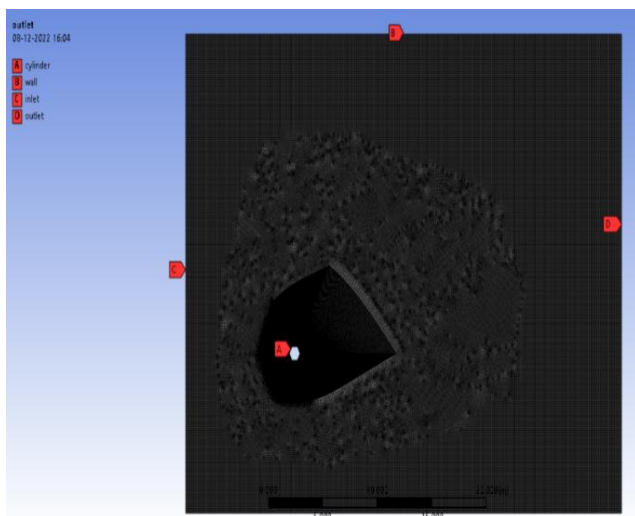


**Figure 3** Meshed Model used in this study

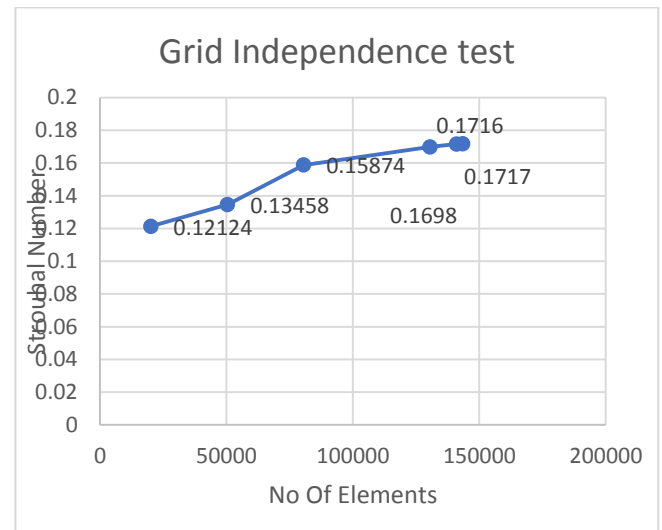


**Chart 1** Variation of Strouhal number with number of elements in mesh

### 2.3 Methodology

The direction of fluid flow is in the positive X-direction, i.e. from left to right. There is a specified uniform inflow velocity  $u = u_0$  selected in accordance with the Reynold number. After that, the system is resolved utilising the formulas of (SST k-) turbulence model. The Navier-Stokes equations in 2D incompressibility are the governing equations. The computational domain identifies the amorphous setting in which the solution is computed. It is made up of a wall, a hexagonal cylinder, a velocity entrance, and a pressure outlet.

Density -  $1 \text{ kg/m}^3$  ;

Viscosity -  $1 \text{ kg/m-s}$

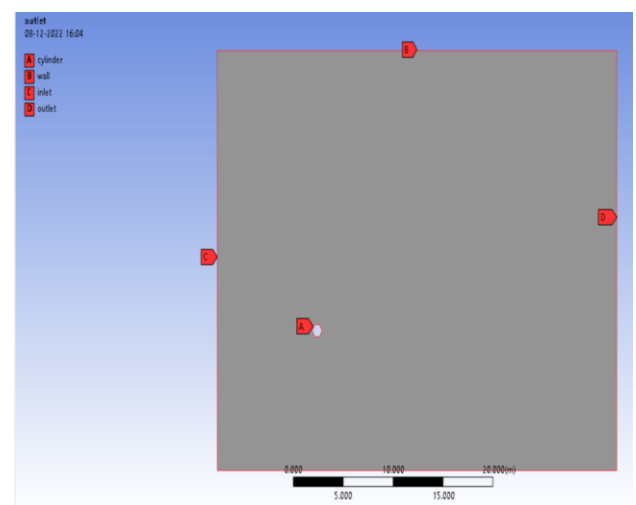


**Figure 4** Schematic of boundary conditions for studying the flow past hexagonal cylinder

## 2.4 Comparison between current and the published results

Based on the mesh grid sensitivity result and validation of present mesh result with that of Khaledi Andersson work, the mesh with 143505 grid elements was selected for present study .

Sr. No	Cylinder Type	Reynold Number	Khaledi & Andersson [2011] St	Present Work [2022] St
1	Hexagonal	100	0.1585	0.1594
2	Hexagonal	500	0.1718	0.177
3	Hexagonal	1000	0.1718	0.175

**Table 1** Comparison of Strouhal number of present work with published work

## 3. Result And Discussion

### 3.1 Drag and lift Variation with Reynold number

The dimensionless coefficients Cd and Cl are used to quantify the drag coefficient and lift coefficient respectively. Graph 2 and 3 shows the variation of drag with Reynold number and variation of lift with Reynold number respectively. An increase in drag and lift coefficient could be evidently seen with an increase in Reynold number.

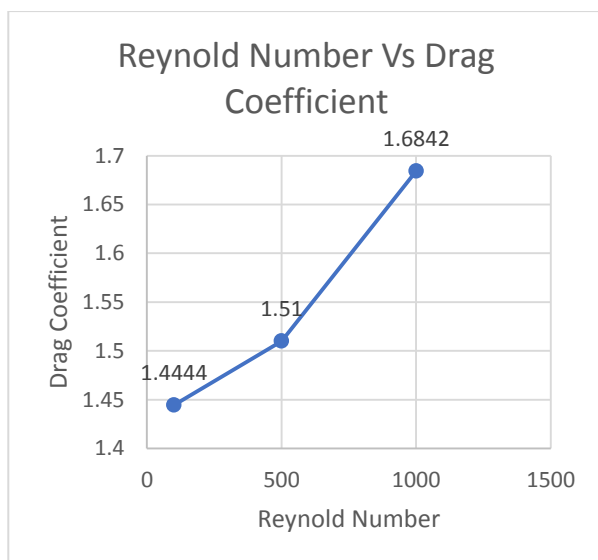


**Chart 2** Drag variation with Reynold number

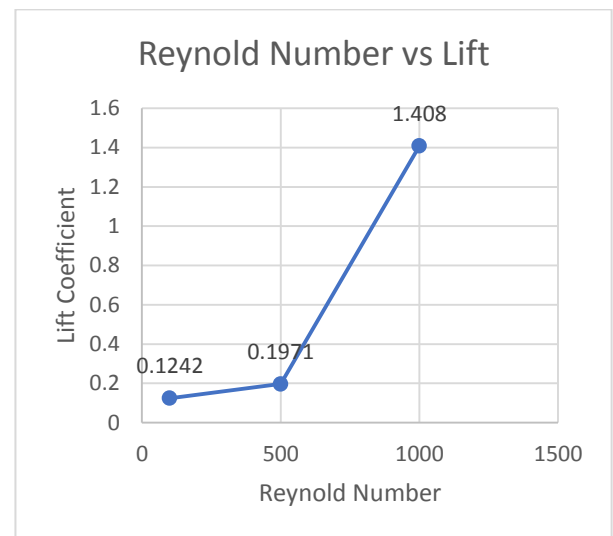


**Chart 3** Lift variation with Reynold number

### 3.2 Velocity Contour, Velocity Streamlines And Pressure Contours

The velocity contours are represented in figures 5 to 7 , whereas pressure contours are represented in figures 8 to 10 . When used to visualise the flow in 2D, velocity contours make it simple to grasp how the air is moving around the cluster of cylinders and how its velocity is changing. The pressure contour allows one to comprehend the coefficient of pressure distribution visually. for the hexagonal cylinder for Re =100,500 and 1000 respectively. According to the scale on the left, the colours red and orange denote higher pressure, while the colours green, yellow, and blue denote relatively lower pressure zones.

Fig.5 illustrates that the base region's generated vortices are alternatively shed and build a laminar vortex street with a Karman-like structure throughout the flow domain. However, at Re equal to 500, the flow-parallel faces appear to be the location where the shear layers appear to divide. And as Reynold number is increased further complete turbulence in wake could be marked.

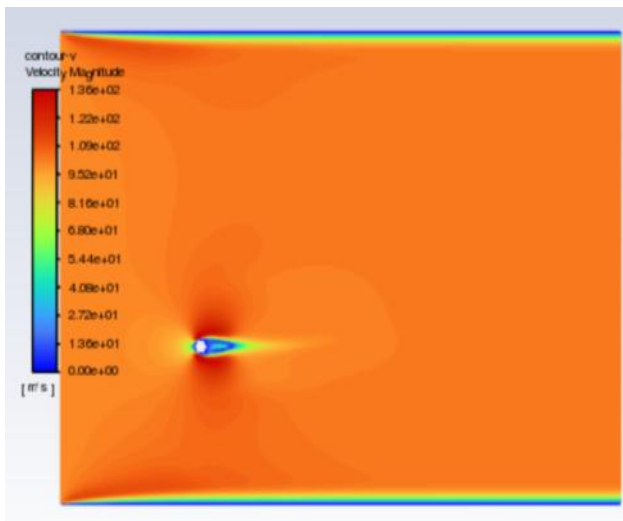


Figure 5 Velocity contour for 100 Re

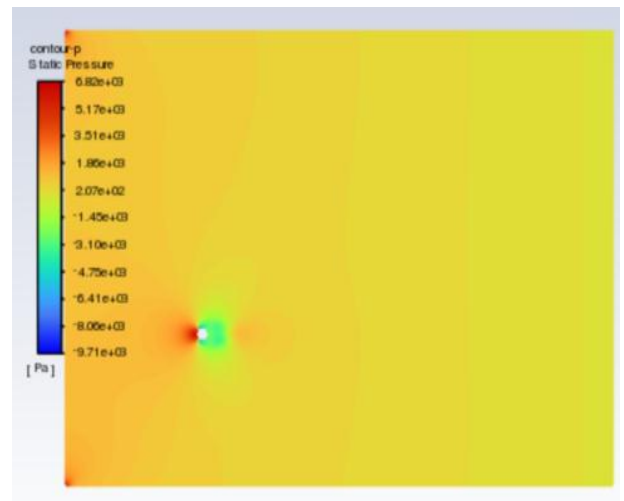


Figure 8 Pressure contour for 100 Re

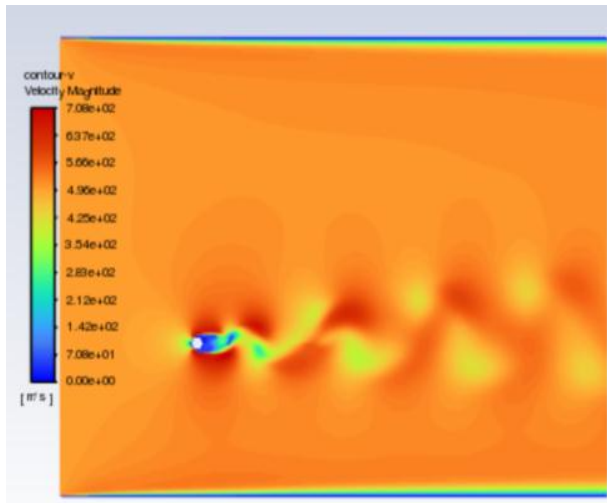


Figure 6 Velocity contour for 500 Re

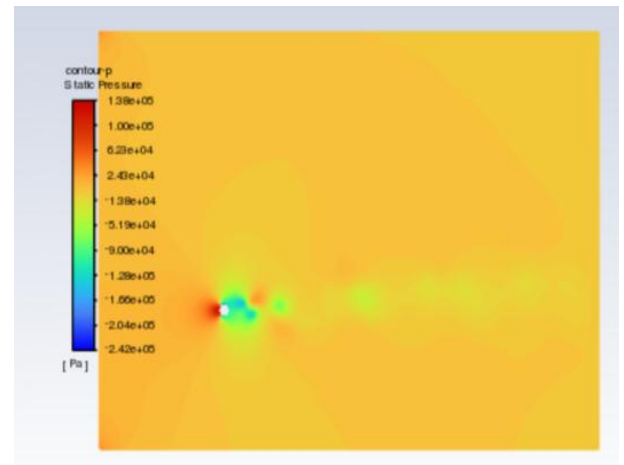


Figure 9 Pressure contour for 500 Re

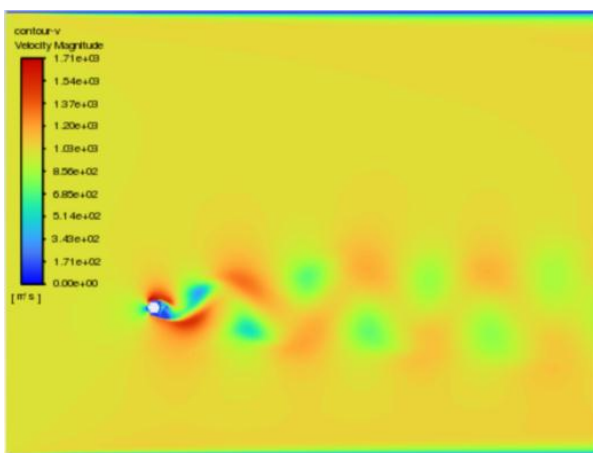


Figure 7 Velocity contour for 1000 Re

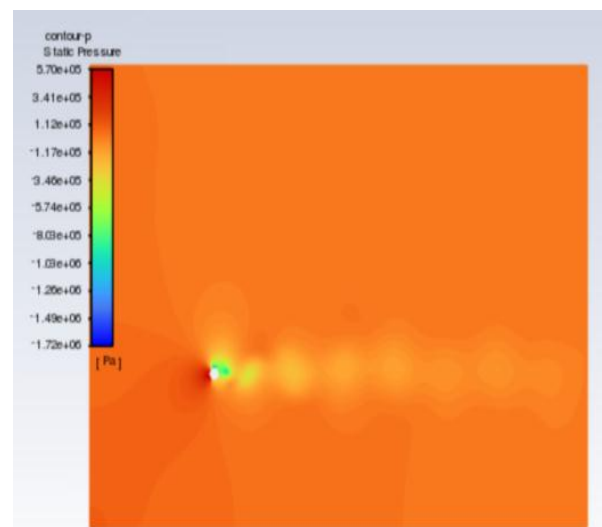


Figure 10 Pressure contour for 1000 Re

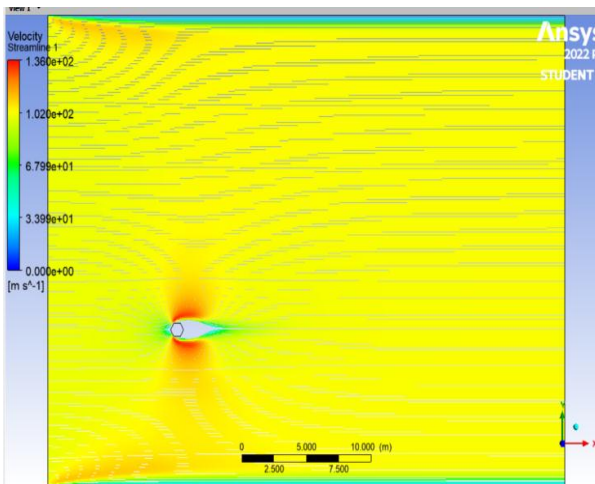


Figure 11 Velocity Streamline for 100 Re

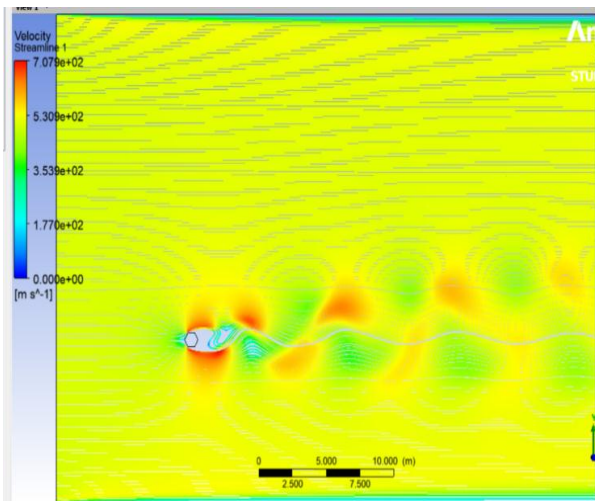


Figure 12 Velocity Streamline for 500 Re

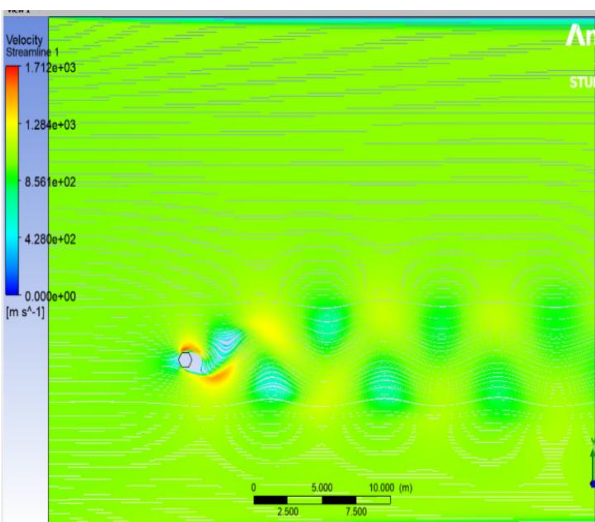


Figure 13 Velocity Streamline for 1000 Re

### 3.3 Strouhal number and frequency Variation with Reynold Number

With increasing Reynolds number, a significant rise in Strouhal number is seen. And also a significant increase in shedding frequency was observed with increase in Reynolds number.

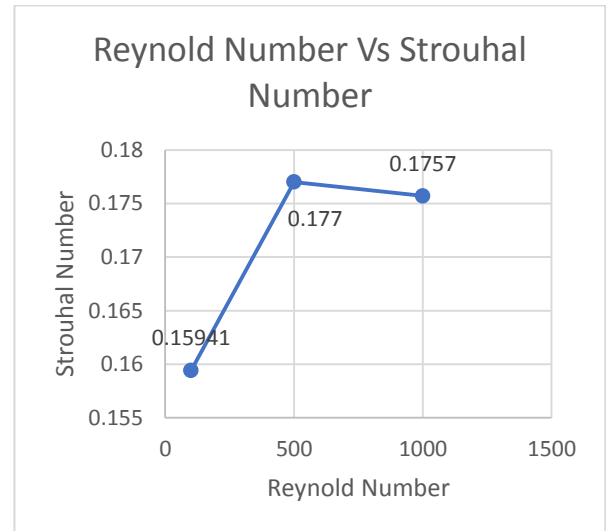


Chart 4 Strouhal Number Variation with Reynolds Number

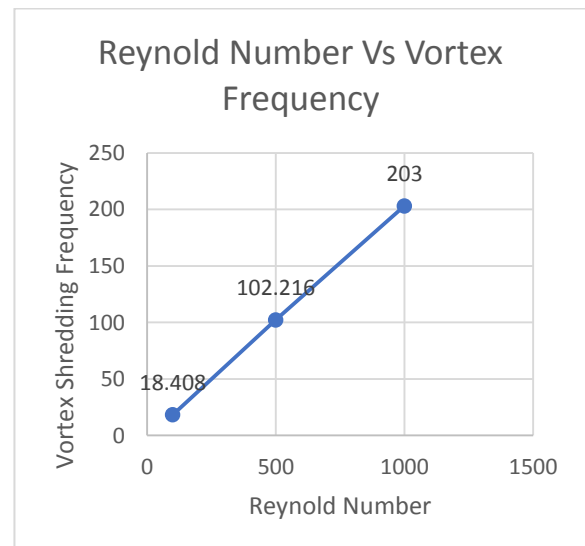


Chart 5 Vortex frequency Variation with Reynold Number

### 4. Conclusion

In this work a two dimensional hexagonal cylinder with corner orientation was analysed using Ansys2022 R1. The computational model was based on the 2D RANS [Reynolds Averaged Navier Stokes Equation] and CFD

formulation was based on SST  $k-\omega$  model. And we found a significant increase in shedding frequency with increase in Reynold number and also with increasing Reynolds number, a significant rise in Strouhal number was marked.

## 5. References

- 1] BLOOR, M. S. 1965. The transition to turbulence in the wake of a circular cylinder. *Journal of Fluid Mechanics*, 19, 290
- 2] ZDRAVKOVICH, M. M. 1997 *Flow Around Circular Cylinders*, vol. 1. Oxford University Press.
- 3] FEY, U., KÖNIG, M. & ECKELMANN, H. 1998. A new Strouhal-Reynolds-number relationship for the circular cylinder in the range 47. *Physics of Fluids*, 10, 1547-1549.
- 4] SOHANKAR, A., NORBERG, C. & DAVIDSON, L. 1998. Low-Reynolds-number flow around a square cylinder at incidence: study of blockage, onset of vortex shedding and outlet boundary condition. *International journal for numerical methods in fluids*, 26, 39-56
- 5] SUMER B.M., F. J. 2006. *Hydrodynamics around cylindrical structures*, World Scientific Publishing Co Pte. Ltd. Singapore.
- 6] VADA, T., NESTEGRD, A. & SKOMEDAL, N. 1989. Simulation of viscous flow around a circular cylinder in the boundary layer near a wall. *Journal of fluids and structures*, 3, 579-594
- 7] TIAN, Z. W. & WU, Z. N. 2009. A study of two-dimensional flow past regular polygons via conformal mapping. *Journal of Fluid Mechanics*, 628, 121-154.
- 8] KHALEDI, H. A. & ANDERSSON, H. I. 2011. On vortex shedding from a hexagonal cylinder. *Physics Letters A*, 375, 4007-4021.